Journal of Computational Electronics X:YYY-ZZZ,200?
©2006 Springer Science Business Media, Inc. *Manufactured in The Netherlands*

Simulation of the Rashba Effect in a Multiband Quantum Structure

OMAR MORANDI
Dipartimento di Elettronica e Telecomunicazioni, Università degli Studi di Firenze,
Via S. Marta 3, I-50139 Firenze, Italy
omar.morandi@unifi.it

LUCIO DEMEIO
Dipartimento di Scienze Matematiche, Università Politecnica delle Marche,
Via Brecce Bianche 1, I-60131 Ancona, Italy
l.demeio@univpm.it

Abstract. The aim of this work is to present an extension of the "kp" multiband model derived in [4], to include the description of the degenerate bands and the spin-orbit coupling, and its application to some spin-sensitive devices. The model is derived within the usual Bloch-Wannier formalism by a k-expansion, and it is applied to calculate the spin dependent transmission coefficients for an asymmetric resonant interband diode.

Keywords: Multiband quantum transport, Rashba effect.

1. Introduction

In recent years, much interest has been devoted to the investigation of spin phenomena in semiconductors. Various devices containing asymmetric quantum wells, where quantized states are spin-split by the Rashba effect, have already been proposed and the properties of such devices have been analyzed from a theoretical point of view [1, 2]. The mixing of valence and conduction bands at the interfaces makes a many-band treatment necessary and, in particular, requires a realistic description of the degenerate valence-band edge.

In this work we propose a new model derived within the usual Bloch-Wannier formalism by a k-expansion. The effective-mass equations are based on an invariant expansion of the valence-band Hamiltonian, which is intimately related to the symmetry of the diamond lattice [3]. We present the six-band version of our model, which gives a full description of the coupling between the conduction and the valence band for the most common semiconductors. In particular, this model generalizes the model derived in [4] to include the description of the degenerate bands and the spin-orbit coupling.

The paper is organized as follows. In Section 2 we discuss the derivation of the model and the approximations employed; Section 3 describes the transparent boundary conditions and in Section 4 we present our numerical results for an asymmetric resonant interband tunneling diode.

2. Multiband envelope function model

We consider an electron of mass m_0 moving in a periodic potential V_L and subject to an additional external potential U which is treated as a perturbation. The Hamiltonian which governs the motion of the electron is given by

$$\mathcal{H} = \mathcal{H}_0 + U(\mathbf{r}) - i\zeta\left(\nabla U(\mathbf{r}) \wedge \nabla\right)\cdot\boldsymbol{\sigma} \qquad (1)$$

where

$$\mathcal{H}_0 = -\frac{\hbar^2}{2m_0}\nabla^2 + V_L(\mathbf{r}) - i\zeta\left(\nabla V_L(\mathbf{r}) \wedge \nabla\right)\cdot\boldsymbol{\sigma}, \quad (2)$$

$\zeta = \hbar^2/(4m_0^2c^2)$, and $\boldsymbol{\sigma}$ is a vector of matrices whose components are the Pauli spin matrices.

It is well know that the eigenfunctions of the unperturbed Hamiltonian $\mathcal{H}_0$ are the Bloch functions $\psi_n^\alpha(\mathbf{k},\sigma,\mathbf{r})$, which can be written as $\psi_n^\alpha(\mathbf{k},\sigma,\mathbf{r}) = \mathrm{e}^{i\mathbf{k}\cdot\mathbf{r}} u_n^\alpha(\mathbf{k},\sigma,\mathbf{r})$, where the $u_n^\alpha(\mathbf{k},\sigma,\mathbf{r})$ have the same periodicity properties of the crystal lattice and form a complete set with respect to periodic functions. Also, with $E_n^\sigma(\mathbf{k})$ we indicate the energy bands, with the index n denoting the bands and α running over the possible n_α degenerate states related to the eigenvalue E_n. Finally, the index σ labels the spin of the electron, with $\sigma = +,-$ for the spin up and spin down components respectively.

The aim of the "kp" approach is to separate the fast oscillating contribution to the Hamiltonian, given by the periodic potential V_L, from the slower contribution, which models the lattice stress, the variabile chemical composition of the alloy and other factors, and which is represented in our model by the external potential U. This is achieved by a suitable averaging procedure of the equations of motion over each lattice cell. More specifically, we assume that $U(\mathbf{r})$ is almost constant on a lattice cell; this is equivalent to the approximation [4, 5]

$$\left\langle \psi_{n,\mathbf{k}}^{\alpha,\sigma} \,|\, U \,|\, \psi_{n',\mathbf{k}'}^{\alpha',\sigma'} \right\rangle \simeq \tilde{U}(\mathbf{k}-\mathbf{k}') \left\langle u_{n,\mathbf{k}}^{\alpha,\sigma} \,|\, u_{n',\mathbf{k}'}^{\alpha',\sigma'} \right\rangle \quad (3)$$

where is the Fourier transform of $U(\mathbf{r})$.

The evolution of the electron wave function $\Psi(\mathbf{r},t)$ is determined by the Schrödinger equation with the perturbed Hamiltonian $\mathcal{H}$. By expanding the wave function in the Bloch basis,

$$\Psi(\mathbf{r}) = \sum_{n,\alpha,\sigma} \int_B \varphi_n^\alpha(\mathbf{k},\sigma)\, \psi_n^\alpha(\mathbf{k},\sigma,\mathbf{r})\, \mathrm{d}\mathbf{k}, \qquad (4)$$

where B indicates the first Brillouin zone, the following equation is obtained for the expansion coefficients:

$$\begin{aligned} i\hbar \frac{\partial \varphi_n^\alpha(\mathbf{k},\sigma)}{\partial t} &= E_n^\sigma(\mathbf{k})\, \varphi_n^\alpha(\mathbf{k},\sigma) \qquad (5)\\ &+ \sum_{\substack{n'\neq n,\\ \alpha',\sigma'}} \int_B \left\{ \left\langle \psi_{n,\mathbf{k}}^{\alpha,\sigma} \,|\, U \,|\, \psi_{n',\mathbf{k}'}^{\alpha',\sigma'} \right\rangle \varphi_{n'}^{\alpha'}(\mathbf{k}',\sigma') \right.\\ &\left. -i\zeta \left\langle \psi_{n,\mathbf{k}}^{\alpha,\sigma} \,|\, (\nabla U \wedge \nabla)\cdot\boldsymbol{\sigma} \,|\, \psi_{n',\mathbf{k}'}^{\alpha',\sigma'} \right\rangle \varphi_{n'}^{\alpha'}(\mathbf{k}',\sigma') \right\} \mathrm{d}\mathbf{k}'. \end{aligned}$$

By using equation (3), and by following [4] in order to evaluate the scalar products between Bloch functions, we obtain [7]

$$\begin{aligned} i\hbar \frac{\partial \varphi_n^\alpha(\mathbf{k},\sigma)}{\partial t} &= E_n^\sigma(\mathbf{k})\, \varphi_n^\alpha(\mathbf{k},\sigma) \qquad (6)\\ &+ \frac{\hbar}{m_0} \sum_{\substack{n'\neq n,\\ \alpha',\sigma'}} \int_B \tilde{U}(\mathbf{k}-\mathbf{k}')(\mathbf{k}-\mathbf{k}')\cdot\mathbf{Q}\, \varphi_{n'}^{\alpha'}(\mathbf{k}',\sigma')\, \mathrm{d}\mathbf{k}, \end{aligned}$$

where

$$\begin{aligned} \mathbf{Q} &= \frac{\boldsymbol{\pi}_{n,n'}^{\alpha,\alpha'}(\mathbf{k},\mathbf{k}',\sigma,\sigma')}{\Delta E_{nn'}^{\sigma,\sigma'}(\mathbf{k},\mathbf{k}')} + i\zeta\mathbf{k}' \wedge \left\langle u_{n,\mathbf{k}}^{\alpha,\sigma} \middle| \boldsymbol{\sigma} \middle| u_{n',\mathbf{k}'}^{\alpha',\sigma'} \right\rangle \\ &+ i\frac{\zeta}{\hbar} \left\langle u_{n,\mathbf{k}}^{\alpha,\sigma} \middle| \hat{\mathbf{p}} \wedge \boldsymbol{\sigma} \middle| u_{n',\mathbf{k}'}^{\alpha',\sigma'} \right\rangle, \end{aligned}$$

with

$$\begin{aligned} &\boldsymbol{\pi}_{n,n'}^{\alpha,\alpha'}(\mathbf{k},\mathbf{k}',\sigma,\sigma') = \qquad (7)\\ &\left\langle u_{n,\mathbf{k}}^{\alpha,\sigma} \middle| \hat{\mathbf{p}} + \frac{\hbar}{4m_0c^2}\, (\boldsymbol{\sigma}\wedge\nabla V_L) \middle| u_{n',\mathbf{k}'}^{\alpha',\sigma'} \right\rangle \end{aligned}$$

and

$$\Delta E_{nn'}^{\sigma,\sigma'}(\mathbf{k},\mathbf{k}') = E_n^\sigma(\mathbf{k}) - E_{n'}^{\sigma'}(\mathbf{k}') - \frac{\hbar^2}{2m_0}\left(k^2 - k'^2\right). \qquad (8)$$

At this point, we introduce the approximations of the "kp" theory, in which the quasi-momentum $\mathbf{k}$ acts as a smallness parameter [6]. For the sake of simplicity, we assume that all energy bands attain their maximum or their minimum at $\boldsymbol{k}_0 = 0$. By expanding equation (6) to first order with respect to $|\mathbf{k}|$ and by taking the Fourier transform, we obtain [7]

$$\begin{aligned} i\hbar \frac{\partial \varphi_n^\alpha(\mathbf{r},\sigma)}{\partial t} &= E_n^\sigma(-i\hbar\nabla)\, \varphi_n^\alpha(\mathbf{r},\sigma) \qquad (9)\\ &-i\frac{\hbar\Omega}{m_0} \sum_{\substack{n'\neq n,\\ \alpha',\sigma'}} \nabla U(\mathbf{r}) \cdot \frac{\boldsymbol{\pi}_{n,n'}^{\alpha,\alpha'}(\mathbf{0},\mathbf{0},\sigma,\sigma')}{\Delta E_{n,n'}^{\sigma,\sigma'}(\mathbf{0},\mathbf{0})}\, \varphi_{n'}^{\alpha'}(\mathbf{r},\sigma')\\ &-i\zeta \sum_{\substack{n'\neq n,\\ \alpha',\sigma'}} \nabla U(\mathbf{r}) \cdot \left\langle u_{n,0}^{\alpha,\sigma} \middle| \boldsymbol{\sigma} \middle| u_{n',0}^{\alpha',\sigma'} \right\rangle \wedge \nabla\, \varphi_{n'}^{\alpha'}(\mathbf{r},\sigma')\\ &+\frac{\zeta}{\hbar} \sum_{\substack{n'\neq n,\\ \alpha',\sigma'}} \nabla U(\mathbf{r}) \cdot \left\langle u_{n,0}^{\alpha,\sigma} \middle| \hat{\mathbf{p}} \wedge \boldsymbol{\sigma} \middle| u_{n',0}^{\alpha',\sigma'} \right\rangle \varphi_{n'}^{\alpha'}(\mathbf{r},\sigma'). \end{aligned}$$

For the corrections of higher order in $\mathbf{k}$ we refer to [4]. The numerical results presented in Section 4. show that this approximation is well suited to treat the Rashba effect and interband tunneling phenomena.

The symmetry properties of the crystal lattice considerably reduce the number of independent parameters in the previous expressions. Hereafter, we shall refer to semiconductors belonging to the tetrahedral point group symmetry $\mathcal{O}_h$. In particular, we consider the six-band model including the conduction and the light and heavy holes valence bands. The basis elements belong to the irreducible representation of the point groups Γ_6 and Γ_8 for the conduction and valence band respectively. The matrix elements of equation (9) can be easily evaluated by using the Wigner-Eckart theorem (see [3]).

We want to apply our model to layered heterostructures, where the relevant quantum effects act only along the growth axis; by taking the y coordinate along the growth axis, we have $U(\mathbf{r}) = U(y)$ and $\boldsymbol{\varphi}(\mathbf{r}) = \boldsymbol{\varphi}(y)e^{ik_\perp \cdot \mathbf{r}}$, where $k_\perp$ is the trasverse momentum, which is conserved. Furthermore, we choose the spin axis on the transverse plane and orthogonal to the transverse momentum $k_\perp$. It has been proved that this is the direction where the spin splitting is more evident. For sake of simplicity, we take $k_\perp = (k_x, 0, 0)$. Because of the cylindrical symmetry of the problem, the results depend only upon $|k_\perp|$ and not upon its orientation.

By introducing the vectors

$$\begin{aligned}\boldsymbol{\varphi}_h(\mathbf{r}) &= \left(\varphi_h^{3/2}, \ \varphi_h^{1/2}, \ \varphi_h^{-1/2}, \ \varphi_h^{-3/2} \right)^T \\ \boldsymbol{\varphi}_c(\mathbf{r}) &= \left(\varphi_c^{+}, \ \varphi_c^{-} \right)^T\end{aligned}$$

and the matrices

$$\begin{aligned}\mathbf{H}_{cc} &= \mathbf{I}_{2\times 2}\left(E_c - E + U - \varepsilon\frac{m_0}{2m_c}\frac{\mathrm{d}^2}{\mathrm{d}y^2}\right) + \zeta k_x \frac{\partial U}{\partial y}\sigma_z \\ \mathbf{H}_{vv} &= \mathbf{I}_{6\times 6}\left(E_v - E + U\right) + \mathbf{I}_h\frac{\varepsilon}{2}\frac{\mathrm{d}^2}{\mathrm{d}y^2} + k_x\zeta\frac{\partial U}{\partial y}\frac{1}{3}J_z^{3/2} \\ \mathbf{H}_{cv} &= \overline{\lambda}\frac{\partial U}{\partial y}T_y,\end{aligned}$$

where with $\mathbf{I}_{n\times n}$ we indicate the $n \times n$ unit matrix,

$$\begin{aligned}\mathbf{I}_h &= \mathrm{diag}\left(\frac{1}{m_{hh}}, \ \frac{1}{m_{lh}}, \ \frac{1}{m_{lh}}, \ \frac{1}{m_{hh}}\right) \\ J_z^{3/2} &= \mathrm{diag}\left(3, \ 1, \ -1, \ -3\right) \\ T_y &= -\frac{i}{3\sqrt{2}}\begin{pmatrix} \sqrt{3} & 0 & 1 & 0 \\ 0 & 1 & 0 & \sqrt{3} \end{pmatrix},\end{aligned}$$

we finally obtain

$$i\hbar\frac{\partial}{\partial t}\begin{pmatrix} \boldsymbol{\varphi}_c \\ \boldsymbol{\varphi}_h \end{pmatrix} = \begin{pmatrix} \mathbf{H}_{cc} & \mathbf{H}_{cv} \\ \mathbf{H}_{cv}^\dagger & \mathbf{H}_{vv} \end{pmatrix}\begin{pmatrix} \boldsymbol{\varphi}_c \\ \boldsymbol{\varphi}_h \end{pmatrix} \qquad (10)$$

The other parameters are defined in Table 1

Symbol	Physical Meaning
m_c	Effective mass in conduction band
m_{lh}, m_{hh}	Light, Heavy holes effective masses
$\lambda = \zeta\frac{\sqrt{3}}{\hbar}P + \frac{\hbar}{m_0}\pi^K$	Interband coupling coefficient
$\pi^K = \frac{3}{\sqrt{2}}\mathbf{e}_z \cdot \boldsymbol{\pi}_{c,h}^{+,1/2}$	Kane momentum
$P = -i\frac{\hbar^2}{m_0}\left\langle \psi_S \left\vert \frac{\partial}{\partial_z} \right\vert \psi_Z \right\rangle$	Kane momentum without spin

Table 1: Physical meaning of symbols defined in this paper.

3. Boundary conditions

We consider the case of an electron beam injected from the left and impacting into the simulations domain. We assume that the incoming electrons are localized in the conduction band and we assume that both spin-up and spin-down directions are present. We also assume that $U(0) = U(L) = 0$ and $E > E_v$. The extension to more general cases is straightforward. With these assumptions, the transparent boundary conditions for the multiband Hamiltonian are (see [8] for the details)

$$\frac{\mathrm{d}}{\mathrm{d}y}\boldsymbol{\varphi}(0) = -i\,\mathbf{K}^i\boldsymbol{\varphi}(0) + \boldsymbol{\iota} \qquad (11)$$

$$\frac{\mathrm{d}}{\mathrm{d}y}\boldsymbol{\varphi}(L) = -i\,\mathbf{K}^t\boldsymbol{\varphi}(L), \qquad (12)$$

where

$$\begin{aligned}\mathbf{K}^r &= \mathrm{diag}\ (q_c, \ q_c, \ ip_{hh}, \ ip_{lh}, \ ip_{lh}, \ ip_{hh}) \\ \mathbf{K}^t &= -\mathrm{diag}\ (q_c, \ q_c, \ ip_{hh}, \ ip_{lh}, \ ip_{lh}, \ ip_{hh}) \\ q_c &= \sqrt{2m_c\left(E - E_c\right)} \\ p_j &= \sqrt{2m_j\left(E - E_v\right)} \quad j = hh, lh,\end{aligned}$$

and we have defined $\boldsymbol{\varphi} = (\boldsymbol{\varphi}_c, \ \boldsymbol{\varphi}_h)^T$, $\boldsymbol{\iota} = (\boldsymbol{\iota}_c, \ \mathbf{0})^T$ and $\boldsymbol{\iota}_c = (1, \ 0)^T$ for the spin-up direction and $\boldsymbol{\iota}_c = (0, \ 1)^T$ for the spin-down direction.

4. Numerical results

We have solved the equations of our multiband envelope function model by using a Runge-Kutta scheme for an asymmetric resonant interband tunneling diode (a-RITD).

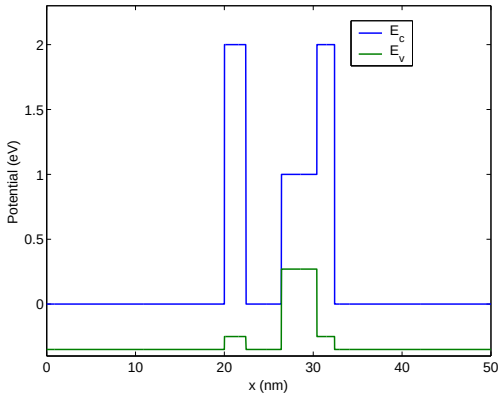

Figure 1: Band alignments of the double barrier structure used in the simulations.

Figure 1 shows the band alignments of the $InAs/AlSb/GaSb/AlSb/InAs$ double barrier structure used in the simulation. The band offset between $InAs$ and $GaSb$ is such that the conduction-band edge of $InAs$ lies $0.15\,eV$ below the energy of the valence-band edge of $GaSb$. Transport through this system involves resonant tunneling of electrons from the $InAs$ emitter, through unoccupied electron states in the subbands of the $GaSb$ well, and subsequently back into the conduction band of the collector.

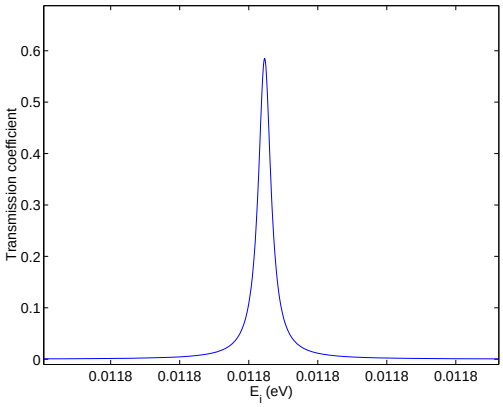

Figure 2: Transmission coefficient for the spin up conduction electrons of the $InAs/GaSb/AlSb$ diode of Fig. 1.

Figure 2 shows the calculated transmission coefficient for the resonant diode for the six band system. The in-plane wave vector is $k_{\|} = \frac{2\pi}{a}(0.03,\, 0,\, 0)$ where a is the lattice constant. The resonant peak is related only to the spin-up conduction electrons, and it disappears completely for the spin-down states. In this way, only conduction electrons injected into the device with resonant energy and with spin parallel to the direction of motion can travel from the emitter to the collector lead; electrons with anti-parallel spin are instead reflected. In Fig. 3 we show the electron density in the valence bands $n_v = \sum_{j=\pm 1/2,\pm 3/2} |\varphi_h^j|^2$ and in the conduction band $n_c = \sum_{j=\pm} |\varphi_c^j|^2$ of spin up electrons with resonant energy. No resonant behaviour is shown by spin down electrons.

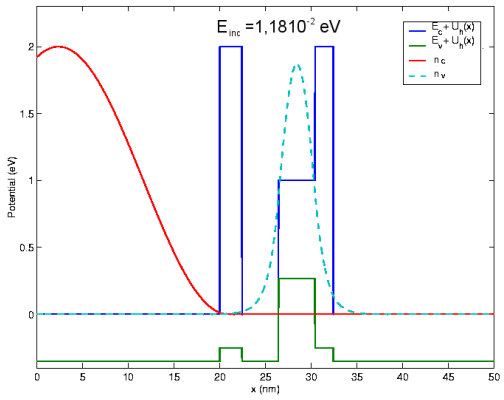

Figure 3: Spin-up electron density at $1.18\,eV$

References

1. M. Altarelli, Phys. Rev. B **28**, 842-845 (1983).
2. D. Z. Y. Ting, E. T. Yu, and T. C. McGill, Phys. Rev. B **45**, 3583-3592 (1992).
3. H. R. Trebin, U. Rössler and R. Ranvaud, Phys. Rev. B **20**, 686-700 (1979).
4. O. Morandi and M. Modugno, Phys. Rev. B **71**, 235331 (2005).
5. B. A. Foreman, Phys. Rev. B **54**, 1909-1921 (1996).
6. J. M. Luttinger and W. Kohn, Phys. Rev. **97**, 869-883 (1955).
7. O. Morandi, PhD Thesis, Università degli Studi di Firenze, April 2006.
8. G. Ali, F. Frosali and O. Morandi, Proc. of the 5-th Int. Workshop on Computing Engineering (SCEE), Capo d'Orlando, Italy, September 5-9, 2004.